INTRA - AND INTER - ANNUAL TRENDS OF SUN-INDUCED FLUORESCENCE (SIF) FOR CONTRASTING VEGETATION TYPES OF INDIA

H. Padalia[1*], S. Kumari[1], S. K. Sinha[1], S. Nandy[1], P. Chauhan[1]

[1]Indian Institute of Remote Sensing, Dehradun-248001, India, hitendra@iirs.gov.in, (shantinayaak, s.sanjivevs)
@gmail.com, (nandy, prakash)@iirs.gov.in

Commission III, WG III/10

KEY WORDS: GOME-2, GPP, NDVI, RAINFALL, SIF, OCO-2

ABSTRACT:

The photosynthesis governs productivity and health of the forests. Traditionally, remote sensing derived reflectance measures have been used to assess forest phenology, productivity and stress. The chlorophyll pigments absorb solar radiation, and emit fluorescence in far red region of electromagnetic spectrum. Chlorophyll fluorescence directly relates to the photosynthetic activity of the plants. Measurement of chlorophyll fluorescence from space has recently been achieved in the form of Sun- Induced Fluorescence (SIF). But SIF response have been found variable with respect to variation in vegetation type, hence, there is a need to study SIF response of tropical forests of India considering their wide extent, contribution to national carbon cycle and climate resilience. In this study, intra- and inter-annual GOME-2 and OCO-2 SIF responses of contrasting Indian tropical forest types *viz.*, dry deciduous (Betul, Madhya Pradesh), moist deciduous (Kalahandi, Orissa) and wet evergreen forests (Uttara Kannada, Karnataka) has been investigated with respect to rainfall, NDVI and GPP trends. The results show that dry, moist and wet forests of India have differences in photosynthetic activity at intra- and inter-annual scale. GOME-2 SIF observations were more variables than OCO-2 SIF, particularly during green-up and senescence phase. SIF explained higher seasonality for dry deciduous followed by moist deciduous and wet evergreen. Annually integrated SIF (proxy of GPP) was in order: wet evergreen>moist deciduous> dry deciduous.

1. INTRODUCTION

Measurements of Sun-Induced Fluorescence (SIF) from space have the potential to improve the accuracy of global photosynthesis maps. Whether a plant is photo-synthetically active or not can be detected directly by capturing the chlorophyll fluorescence radiation through remote sensing techniques. Earlier studies revealed that SIF product can be related with GPP (Lee et al., 2013; Guanter et al., 2014; Frankenberg et al., 2014F). SIF can be expressed by a similar equation in which few assumptions are made that relate with GPP and LUE (Damm et al., 2010; Guanter et al., 2014). Time of acquisition of data has huge impact on the relationship of fluorescence and photosynthetic rate (Tol et al., 2009).

SIF is primarily retrieve through Fraunhofer Line Depth (FLD etc.) by Earth Observation (EO) satellite (Meroni et al., 2009). FLD uses Fraunhofer absorption line that introduced by oxygen band O2B (686nm) and O2A (760nm) (Plascyk, 1975; Moya et al., 2004). At present, global scale SIF retrieved through FLD algorithm is provided by a few satellites like (Global Ozone Monitoring Experiment - 2) and Orbiting Carbon Observatory 2 (OCO-2) with up to a few km (Joiner et al., 2013; Frankenberg et al., 2014). However, these SIF sensors slightly differ with their retrieval channel and sensing time. GOME-2 uses 734nm -758 nm channel (spectra) to detect morning SIF (9: 30 AM, local time) whereas OCO-2 uses 757 & 771 nm channels to retrieve SIF at 1:30 PM (local time).

SIF also vary with different forest type comprises of different canopy structure and biochemical variables. About 90%

variable SIF is governed by canopy structure [LAI (Leaf area index) & LIDFa (leaf inclination distribution factor)] and biochemical variable [(chlorophyll concentration & Vcmax (maximum Carboxylase rate)] (Verrelst et al., 2015, Chen et al., 1999; Tol et al., 2014; Walker et al., 2014). Time-series analysis provides a descriptive feature of seasonality [e.g. ARIMA (auto regressive integrated moving average) model]. Annual SIF variation is estimated by integrating SIF by AUC (area under curve) method (Reed et al., 1994). In present study, we tested the potential of SIF originated at different spectra and time, to capture the seasonality of different forest type induced by photosynthetic activity.

2. METHODOLOGY

2.1 Materials

2.1.1 Satellite SIF Products: GOME-2 SIF (V27 Level 3) monthly data from 2014 to 2017 were downloaded from https://acd-ext.gsfc.nasa.gov/. GOME-2 sensor is a spectrometer on-board European meteorological satellite MetOp-A and MetOp-B, launched in the year 2006 in sun synchronous polar orbit. Its spatial resolution is 40km x 40 km and swath is 1920 km. It senses irradiance in wavelength range 240nm-790nm at 0.5nm spectral resolution (Joiner et al., 2014). OCO-2 SIF product data was downloaded from September 2014 to July 2018 from https://co2.jpl.nasa.gov. OCO-2 is an U.S. environmental science satellite which was launched on 2 July 2014 in sun synchronous orbit. OCO-2 has spatial resolution of 2.25km x 1.29km (Frankenberg et al., 2014). It measures Earth reflected radiation in O2-A band at 0.76 microns and CO2 band

---

* Corresponding author

at 1.61 and 2.06 µm. SIF is retrieval at O2-A band using the SIF emission spectra, ranges between 660 -850nm.

2.1.2 Satellite-derived Biophysical Products: MODIS (MYD13C2) NDVI (Normalised Difference Vegetation Index) 8-days composite product at 0.05° spatial resolution was downloaded from NASA website (https://search.earthdata.nasa.gov). MODIS (MYD17A2H) GPP 8-day composite data of 500m pixel size of 2015-2017 was obtained. GPP products based on fraction of absorbed photosynthetically active radiation (fAPAR) and photosynthetically Active Radiation (PAR) reflectance of vegetation which indicates the productivity of plants.

2.1.3 Ancillary Data: District wise monthly rainfall data (AWS based) of different forested grids belonging to period 2013 to 2017 was downloaded from Indian Meteorological Department (IMD) website (http://www.imd.gov.in/). In addition, the mean annual precipitation and temperature spatial data layers from Worldclim (www.worldclim.org/) was used. Vegetation type map of India was obtained from Reddy et al. (2015).

2.2 Methods

2.2.1 Selection of Contrasting Vegetation Types: According to Koppen-Geiger scheme of classification and based on vegetation type map of India (Reddy et al. 2015), three contrasting vegetation types were chosen i.e. Tropical Dry Deciduous (TDD) from Betul, Madhya Pradesh, Tropical Moist Deciduous (TMD) from Kalahandi, Orissa and Tropical Wet Evergreen (TWE) from Uttara Kannada, Karnataka of India (Figure 1).
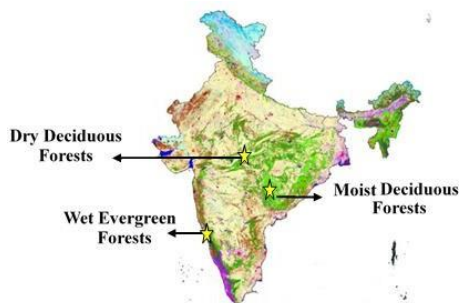

Figure 1. Location of selected forest type in India

The factors such as data availability, species composition, Mean rainfall (MRF), Mean Temperature (MT) (℃) area extent (to suffice GOME-2 pixel extent) and seasonal variation were taken into account for selection of the site within the selected vegetation type (Table 1).

S. No.	Forest Type	Dominant Species	MT (℃)	MRF (mm)
1.	TDD	*Tectona grandis & Butea sp. etc.*	23-29	750 - 1900
2.	TMD	*Shorea robusta & Terminalia sp. etc.*	21- 26	1200- 2000
3.	TWE	*Diptero carpus & Mesua hopea* etc.	24-27	2000- 3000

Table 1. Type of selected forest and their specific characters

2.2.2 Pre-Processing of SIF Data: GOME-2 and OCO-2 SIF SIF data were downloaded in NetCDF (.nc) and NetCDF-4 (.nc4) in 2-D and 1-D data format respectively. NetCDF format can be directly opened in HDF viewer, Panoply, MATLAB and R (CRAN) etc. software. ArcGIS uses "Make NetCDF Raster Layer" tool from ArcTool box to converts 2-D NetCDF file to other raster format (.TIF).

GOME-2 SIF images of Indian region were extracted from the global coverage. However, OCO-2 SIF data global coverage is provided in the form of point layer (1-D). A Python script in Linux was used to extract are OCO-2-point data for Indian region. Negative and no data values were removed from raster layer marking as error or flag.

2.2.3 Intra and Inter-Annual SIF Trend Analysis: Box plot method showing lowest value, highest value, lower quartile, upper quartile, distribution or range and median value were used to show the SIF trends using R studio (CRAN team, 2018). ARIMA (auto regressive integrated moving average) model is used to find out the temporal trend of SIF varying with other variables (e.g. rainfall, NDVI, and GPP) through time series analysis (CRAN team, 2018). In this study trend and point inflection (TPI) methods are used jointly by the help of CRAN-R statistical software (CRAN team, 2018). TPI method permits easy discrimination of growing season having multiple growth seasons. Pre-defined or comparative references value has been used to identify the transition phase (i.e. leaf fall as end of senescence, leaf flush as onset of greenness) as a threshold value. Phenological transition periods is the time lag between two specific phenological conditions.

The inflection point method based on detection of values and point at particular range of time (Reed et al., 1994). Trend derivative methods used to estimate time integrated SIF for inter-annual variation analysis. tSIF estimated by using AUC (Area Under Curve) with quantitative accuracy tests through library (DescTools) available in R- core package. AUC drawn either one of these method "trapezoid", "step" or "spline". "spline" method is used with 'splinefun' function integrate in 'function'. Loess regression is applied to smoothen the time series dataset and then time integrated value is calculated (Figure 2).
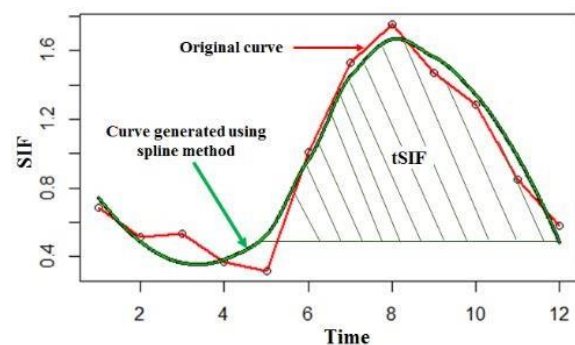

Figure 2. Time integrated SIF (tSIF) smoothened using spline function

2.2.4 Relationship of SIF with Biophysical Parameters: The biophysical parameters impact and pattern on SIF was analysed. Also seasonal as well as spatial variation examined. Partial correlations applied between SIF of GOME-2 and these parameters. The climatic variables are aggregated spatially and distributed monthly for each selected sites of forest. Individual variables relationship is derived and studied. Correlation

coefficient of rainfall ground station point data and GOME-2 SIF is estimated. In this relationship one is ground data i.e. district rainfall IMD data and other one is satellite product. Bias and variance is estimated.

This involves the study of phenological events and relationship during stress as well as growing phase. For this tSIF (time integrated SIF) and tNDVI (time integrated NDVI) values are studied for stress as well as for growing phase. The generated values are compared with each other. To derive GPP relationship with GOME-2 SIF similar above section trend analysis is done. Coefficient of regression value are also generated to compare the relationship of one variable with each other.

3. RESULTS AND DISCUSSION

3.1 Intra-Annual SIF Trend Analysis

Seasonal variations affect the photosynthetic activity by regulating the phenology of forest. Seasonal variation (intra-annual) are shown by box-plot of monthly SIF for tropical dry deciduous, moist deciduous and wet evergreen forest type (Figure 3).
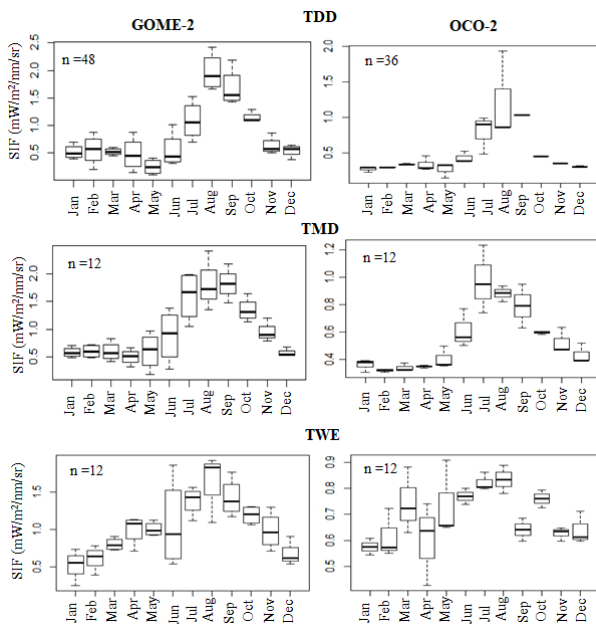

Figure 3. Intra-annual trend of SIF derived from GOME-2 (left) and OCO-2 (right) for different forest type.

3.1.1 Tropical Dry Deciduous (TDD): GOME-2 SIF values show large variation in minimum and maximum values indicating dry deciduous forest undergo minimum as well as maximum period of photosynthetic activity (Figure 3, top). Similar trend is also observed for OCO-2 SIF response with high variability during growth phase i.e., July –August and negligible during senescence. Though both GOME-2 SIF and OCO-2 able to capture the seasonality of dry deciduous forest well, yet GOME-2 SIF response was found tracking seasonal changes more clearly. The variability in SIF in June reaches to a maximum value of more than 1 and minimum value less than 0.5, due to leaf flush resulting into accelerating metabolic activities (Dadhwal et al., 2012) which causes this variation in SIF after leaf emergence.

In July, August & September growth of trees, particularly foliage is maximum with optimum growth condition. The higher metabolic activities of growing phase promote high productivity (Jha et al., 2013) thus account for high SIF values. Senescence phase starts from end of November and the forest remains leafless till March (Shah et al., 2007). To withstand the high temperature and low rainfall, TDD forests shed their leaves that reduces the transpiration rate and helps for their survival (Singh, Kushwaha, 2005). In the month of February and April, due to undergrowth (shrubs and herbs such as grasses) exposure (Pande et al., 2002), they also contribute to SIF showing more variability as compared to January and December.

3.1.2 Tropical Moist Deciduous (TMD): These forests receive rainfall for four to five months. Due to this, the duration of growth phase length is more i.e., May to October. So, the growth is evenly distributed due to prolonged favourable condition for growth resulting into slow growth showing lesser SIF values during growth phase and high during senescence phase as compared to dry deciduous forest (Figure 3, middle). The leaves emerge in this type of forest during May –June. The SIF is quite higher as compared to previous months. The variability in SIF was found high because the selected forest has a mixed forest having different leaf emergence phases for different species found in this forest (Sinha et al., 2017). Peak growth phase of this forest ranges from end of June to October (Singh et al., 1993) which shows high values of SIF all round these months. Variability of SIF is more in the months of June and July due to maximum growth. Senescence phase starts from end of December and the forest remains leafless till March when the flowering starts (Poorter et al., 2007).

3.1.3 Tropical Wet Evergreen (TWE): In the tropical wet evergreen, the seasonal variability do not show any specific trend as compared to dry deciduous and moist deciduous forests as the leaf fall, growth and senescence phases are not separable. For the evergreen vegetation, the SIF values remains uniform throughout the year due to no specific season for leaf fall so they keep on growing all-round the year (Dash et al., 2010). Still during August, it has attained maximum growth with highest value of SIF around 2.0. Minimum photosynthesis in the month of January. Due to metabolic activities throughout the year (Pascal et al., 2004), the variability in SIF is more during all months with a maximum variability in the month of June with highest SIF (Figure 3, bottom). The OCO-2 SIF response deviated from GOME-2 SIF in the month of April and September except these two months, there is similarity between growing as well senescence phase of both the satellite SIF trends.

3.2 Time Series Analysis (Intra- And Inter-Annual SIF)

SIF of three contrasting tropical forest types show different level of photosynthetic activity in different months. Overall mean SIF values for wet evergreen is more as compared to dry and moist deciduous. But maximum SIF response was observed in August for dry deciduous. It indicates that dry deciduous forest have high photosynthetic capacity for short duration (Figure 4).
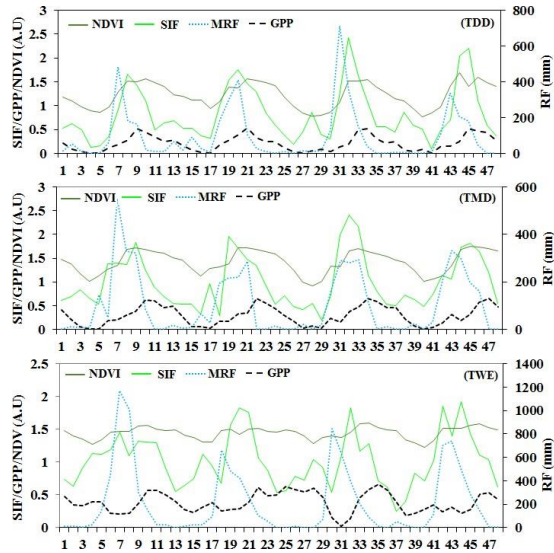
Figure 4. Time- series trends analysis for monthly variable [SIF (GOME-2), GPPMODIS, NDVIMODIS, and Rainfall (RF)] from 2014 to 2017 (n=48).

To predict the seasonal cycle, the SIF derived from GOME-2 served as an effective predictor for different forest types. The trend is more closely corresponded with rainfall and GPP than with NDVI.

3.2.1 Tropical Dry Deciduous (TDD): The pattern and seasonality that are obtained through SIF data are different from traditional vegetation indices records. The SIF & GPP shows enhanced productivity from July to October and values reaches to peak during post monsoon months i.e. August, September and October whereas rainfall is at its peak in the month of June and July. During dry months they shed leaf (April, May, June) so, the SIF, GPP and NDVI reaches to minimum in each year to limit evapotranspiration loss (Singh & Kushwaha,2005). SIF and rainfall shows highest value in the year 2016 whereas NDVI and GPP showing similar trend for all the years. As compared SIF from these three variables the correlation with rainfall is better than other two variables i.e. (R^2=0.62) (Figure 5). SIF relates to GPP and NDVI with R^2 =0.58 and 0.5 respectively (p <0.005).
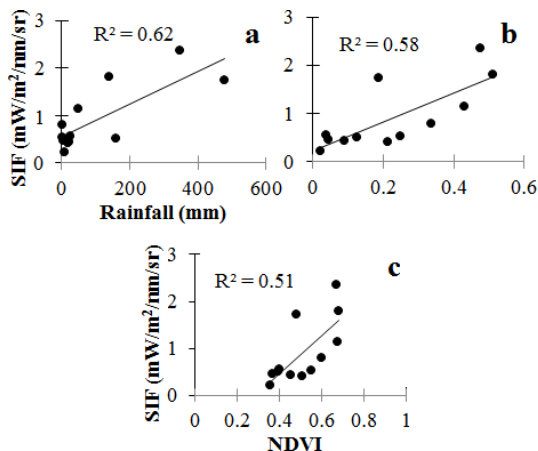

Figure 5. GOME-2 SIF relationship with rainfall (a), GPP (b) and NDVI (c) for TDD

3.2.2 Tropical Moist Deciduous (TMD): SIF shows rapid rise after receiving first shower of rains, i.e. from May which is different while comparing to dry sites which shows rise in value during late June supporting the findings of Sinha et al., (2017). In the year 2016 and 2017 SIF and rainfall follow each other but not in 2014 and 2015. The trend of GPP and NDVI remain same for entire four years whereas SIF reaches to peak value 2.4 during 2016. It was also observed that SIF reacted sharply to increasing rainfall amount during growing phases of forests, more sharply than NDVI. On the other hand, sharp decrease in SIF was observed in post-monsoon period indicating increasing level of water stress in the forests for which NDVI did not show much sensitivity till November months. Rainfall shows highest R^2 with SIF R^2 = 0.55 (p<0.5) for TMD forest (Figure 6). SIF is not well correlated with GPP and NDVIMODIS with R^2=0.4 (p<0.5) for TMD forest.
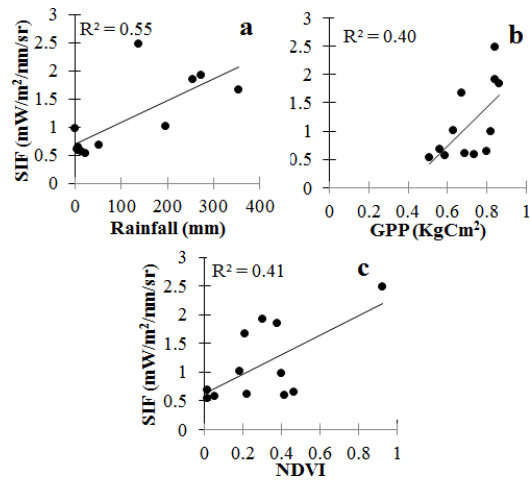

Figure 6. GOME-2 SIF relationship with rainfall (a), GPP (b) and NDVI (c) for TMD

3.2.3 Tropical Wet Evergreen (TWE): The SIF response of TWE is unique. NDVI trend of 2015 did not show seasonal variation (Prasad et al. 2007) but SIF showed seasonal variability for the same period. This shows that SIF is more related to phenology as well as stress in evergreen species than NDVI. The seasonal correlation between SIF and GPP was also weaker in the wet tropics, mostly because of the minimal GPP seasonality and noise in the data (Giardina et al., 2018) (Figure 7).
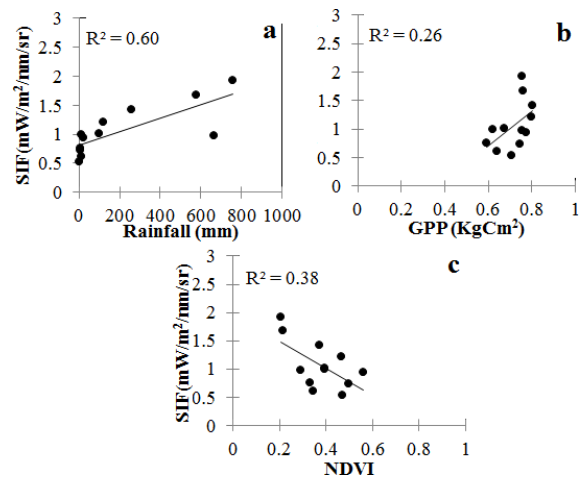

Figure 7. GOME-2 SIF relationship with rainfall (a), GPP (b) and NDVI (c) for TWE

Leaf emergence takes place in February and March (pre-monsoon) and led to rise of SIF value in each year but the same could not captured using NDVI. Flowering and fruiting takes placed in between December-March. Wet evergreen was found less sensitive to precipitation seasonality. As trees in tropical wet evergreen forests contain more biomass and have deep rooting systems which enables to access them deeper soil moisture thus avoid impacts of drought month on photosynthetic capacity.

3.3 Inter-Annual SIF Trend Analysis

Minor differences were observed in the values of yearly tSIF estimated from original curve and smoothened curve by AUC and spline algorithm. The unit of tSIF depend upon the SIF unit (i.e. $mW/m^2/nm/sr$). Overall tSIF (2014-2017) estimated through GOME-2 shows highest for TWE whereas OCO-2 showed tSIF for TMD was slightly higher than TWE (Table 2).

GOME-2						
Year	2014	2015	2016	2017	Mean	SD
TDD	7.98	10.40	9.60	9.50	9.37	0.88
TMD	11.50	10.70	11.80	11.50	11.38	0.41
TWE	12.30	11.90	10.70	12.30	**11.80**	0.66
Mean	10.59	11.00	10.70	**11.10**		
SD	1.88	0.65	0.90	1.18		
OCO-2						
Year	2015	2016	2017	Mean	SD	
TDD	5.07	6.81	5.84	5.91	0.71	
TMD	6.86	5.99	5.98	**6.28**	0.41	
TWE	5.99	6.14	6.64	6.26	0.28	
Mean	5.97	**6.31**	6.15			
SD	0.73	0.36	0.35			

Table 2: Time integrated SIF (tSIF) from GOME-2 and OCO-2

Annual tSIF estimated from GOME-2 (tSIF$_{GOME-2}$) was higher than tSIF from OCO-2 (tSIF$_{OCO-2}$) for almost all year (Table 2). Total tSIF was lowest for TMD forest type than TMD and TWE estimated from both the SIF sensors. tSIF$_{GOME-2}$ of TDD for year 2016 and 2017 is almost same whereas, tSIF$_{OCO-2}$ shows highest value for year 2016 instead of 2015, as rainfall was also recorded higher for the same year. Yet, tSIF for year 2015 shows little anomaly as OCO-2 estimates higher for TMD and lower for TDD and TWE but GOME -2 estimates highest for TDD than TMD and TWE. TWE shows highest photosynthetic activity than TMD and TDD forest type.

The dry deciduous and moist deciduous forest revealed similar trends in both SIF and NDVI but wet evergreen forest exhibited more prominent differences in SIF and NDVI (Figure 8). This is because SIF is associated with chlorophyll molecules function (Frankenberg et al., 2014) and not only greenness of leaf whereas NDVI rely only on greenness of leaf (Anyamba et al., 2001).
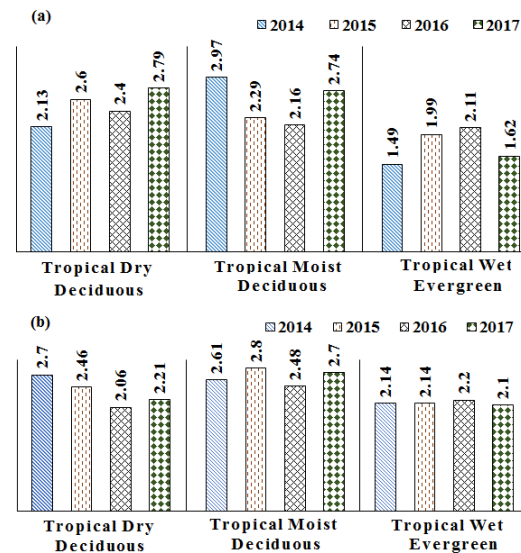

Figure 8. Illustration of pattern difference using (a) SIF & (b) NDVI values

4. CONCLUSION

GOME-2 SIF observations efficiently captured the seasonal variability than OCO-2 SIF. Estimated monthly SIF and annual tSIF are guided by the rainfall for all forest type. Observation shows that, SIF effectively captures the photosynthetic variability linked with leaf transition periods (i.e. leaf flushing and senescence phase) particularly in dry deciduous forest. Monthly SIF also shows unique characteristic of dry deciduous forest with a peak and deep annually. SIF potentially captures seasonality while NDVI gets saturated specially in evergreen forest. Annual tSIF as a proxy of photosynthetic activity (i.e. GPP) shows, wet evergreen forest sequestrated more carbon than moist deciduous and dry deciduous forest. GPP from MODIS can be replaced by tower generated GPP to get a more accuracy in terms of relation. In future, SIF can be used as an important tool to measure temporal and spatial variability of photosynthetic activity, stress pattern, and forest health of different forest type.

ACKNOWLEDGEMENTS

REFERENCES

Anyamba, A., Tucker, C. J., Eastman, J. R., 2001. NDVI anomaly patterns over Africa during the 1997/98 ENSO warm event. *Int. J. Remote Sens.*, *22*(10), 1847-1860.

Chen, J.., Liu, J., Cihlar, J., Goulden, M.., 1999. Daily canopy photosynthesis model through temporal and spatial scaling for remote sensing applications. Ecol. Modell. 124, 99–119. https://doi.org/10.1016/S0304-3800(99)00156-8

Dadhwal, V. K., 2012. Assessment of Indian carbon cycle components using earth observation systems and ground

inventory. *Int Arch Photogram Remote Sens Spat Inform Sci,* 39, 249-254.

Damm, A., Guanter, L., Paul-Limoges, E., van der Tol, C., Hueni, A., Buchmann, N., Eugster, W., Ammann, C., Schaepman, M.E., 2015. Far-red sun-induced chlorophyll fluorescence shows ecosystem-specific relationships to gross primary production: An assessment based on observational and modeling approaches. *Remote Sens. Environ.* 166, 91–105. https://doi.org/10.1016/j.rse.2015.06.004

Guanter, L., Zhang, Y., Jung, M., Joiner, J., Voigt, M., Berry, J.A., Frankenberg, C., Huete, A.R., Zarco-Tejada, P., Lee, J.E., Moran, M.S., Ponce-Campos, G., Beer, C., Camps-Valls, G., Buchmann, N., Gianelle, D., Klumpp, K., Cescatti, A., Baker, J.M., Griffis, T.J., 2014b. Global and time-resolved monitoring of crop photosynthesis with chlorophyll fluorescence. *Proc. Natl. Acad. Sci.* U. S. A. 111. https://doi.org/10.1073/pnas.1320008111

Dash, J., Jeganathan, C., Atkinson, P. M., 2010. The use of MERIS Terrestrial Chlorophyll Index to study spatio-temporal variation in vegetation phenology over India. *Remote Sens. Environ.* 114(7), 1388-1402.

Frankenberg, C., Dell, C.O., Berry, J., Guanter, L., Joiner, J., Köhler, P., Pollock, R., Taylor, T.E., 2014.Remote Sensing of Environment Prospects for chlorophyll fluorescence remote sensing from the Orbiting Carbon Observatory-2. *Remote Sens. Environ.* 147, 1–12. https://doi.org/10.1016/j.rse.2014.02.007

.

Jha, C. S., Thumaty, K. C., Rodda, S. R., Sonakia, A., Dadhwal, V. K., 2013. Analysis of carbon dioxide, water vapour and energy fluxes over an Indian teak mixed deciduous forest for winter and summer months using eddy covariance technique. *J. Earth Syst. Sci.*, 122(5), 1259-1268.

Joiner, J., Guanter, L., Lindstrot, R., Voigt, M., Vasilkov, A.P., Middleton, E.M., Huemmrich, K.F., Yoshida, Y., 2013. Global monitoring of terrestrial chlorophyll fluorescence from moderate-spectral-resolution near-infrared satellite measurements : methodology, simulations, and application to GOME-2. *Atmos. Meas.* 6, 2803–2823. https://doi.org/10.5194/amt-6-2803-2013

Joiner, J., Yoshida, Y., Guanter, L., Lindstrot, R., Voigt, M., Jung, M., Vasilkov, A., Middleton, E., Huemmrich, K.F., Tucker, C.J., Frankenberg, C., Berry, J.A., Schaefer, K., Koehler, P., 2014. New Measurements of Chlorophyll Fluorescence with Gome-2 and Comparisons with the Seasonal Cycle of Gpp from Flux Towers. *5th Int. Work. Remote Sens. Veg. Fluoresc.* 7–11.

Lee, J.-E., Frankenberg, C., van der Tol, C., Berry, J.A., Guanter, L., Boyce, C.K., Fisher, J.B., Morrow, E., Worden, J.R., Asefi, S., Badgley, G., Saatchi, S., 2013. Forest productivity and water stress in Amazonia: observations from GOSAT chlorophyll fluorescence. *Proc. R. Soc. B Biol. Sci.* 280, 20130171–20130171. https://doi.org/10.1098/rspb.2013.0171

Meroni, M., Rossini, M., Guanter, L., Alonso, L., Rascher, U., Colombo, R., Moreno, J., 2009. Remote sensing of solar-induced chlorophyll fluorescence: Review of methods and applications. *Remote Sens. Environ*. 113, 2037–2051. https://doi.org/10.1016/j.rse.2009.05.003

Moya, I., Camenen, L., Evain, S., Goulas, Y., Cerovic, Z.G., Latouche, G., Flexas, J., Ounis, A., 2004. A new instrument for passive remote sensing: 1. Measurements of sunlight-induced chlorophyll fluorescence. *Remote Sens. Environ.,* 91, 186–197. https://doi.org/10.1016/j.rse.2004.02.012

Pande, P. K., Meshram, P. B., Banerjee, S. K., 2002. Litter production and nutrient return in tropical dry deciduous teak forests of Satpura plateau in central India. *Trop. Ecol.*, *43*(2), 337-344.

Pascal, J. P., Ramesh, B. R., Franceschi, D. D., 2004. Wet evergreen forest types of the southern Western Ghats, India. *Trop. Ecol.*, *45* (2), 281-292.

Patel, N. R., Padalia, H., Devadas, R., Huete, A., Kumar, A. S., Krishna Murthy, Y. V. N., 2018. Estimating net primary productivity of croplands in Indo-Gangetic Plains using GOME-2 sun-induced fluorescence and MODIS NDVI. *Curr. Sci.* (00113891), 114(6).

Plascyk, J.A., 1975. The MK II Fraunhofer Line Discriminator (FLD-II) The MK II Fraunhofer Line Discriminator (FLD -II) for Airborne and Orbital Remote Sensing of Solar-Stimulated Luminescence. *optical Eng.* 14, 339–346. https://doi.org/10.1117/12.7971842

Poorter, L., Kitajima, K., 2007. Carbohydrate storage and light requirements of tropical moist and dry forest tree species. *Ecology*, *88*(4), 1000-1011.

Prasad, V. K., Badarinath, K. V. S., Eaturu, A., 2007. Spatial patterns of vegetation phenology metrics and related climatic controls of eight contrasting forest types in India–analysis from remote sensing datasets. *Theor. Appl. Climatol.*, *89*(1-2), 95.

R Core Team, 2018. R: A language and environment for statistical computing. *R Foundation for Statistical Computing*, Vienna, Austria. URL http://www.R-project.org/.

Reed, B. C., Brown, J. F., VanderZee, D., Loveland, T. R., Merchant, J. W., Ohlen, D. O., 1994. Measuring phenological variability from satellite imagery. *J. veg. sci.,* 5(5), 703-714.

Reddy, C. S., Jha, C. S., Diwakar, P. G., Dadhwal, V. K., 2015. Nationwide classification of forest types of India using remote sensing and GIS. *Environ. Moni. Assess*. 187(12), 777.

Singh, K. P., Kushwaha, C. P., 2005. Paradox of leaf phenology: Shorea robusta is a semi-evergreen species in tropical dry deciduous forests in India. *Curr. Sci.*, 88, 1820−1824.

Shah, S. K., Bhattacharyya, A., Chaudhary, V., 2007. Reconstruction of June–September precipitation based on tree-ring data of teak (Tectona grandis L.) from Hoshangabad, Madhya Pradesh, India. *Dendrochronologia*, *25*(1), 57-64.

Giardina, F., Konings, A. G., Kennedy, D., Alemohammad, S. H., Oliveira, R. S., Uriarte, M., Gentine, P., 2018. Tall Amazonian forests are less sensitive to precipitation variability. *Nat. Geosci.,* 11, 405–409. https://doi.org/10.1038/s41561-018-0133-5

Singh, O., Sharma, D. C. Rawat, J. K., 1993. Production and decomposition of leaf litter in sal, teak, eucalyptus and poplar forests in Uttar Pradesh. *Indian For.*, 119(2), 112–121.

Sinha, S. K., Padalia, H., Kumar, A. S., 2017. Space-borne sun- induced fluorescence: an advanced probe to monitor seasonality of dry and moist tropical forest sites. *Curr. Sci.*, *113*(11), 2180.

Tol, C. van der, Berry, J.A., Campbell, P.K.E., Rascher, U., 2014. Models of fluorescence and photosynthesis for interpreting measurements of solar-induced chlorophyll fluorescence. J. Geophys. Res. *Biogeosciences*, 119, 2312–2327. https://doi.org/10.1002/2014JG002713.We

Tol, C. van der., Verhoef, W., Rosema, A., 2009. A model for chlorophyll fluorescence and photosynthesis at leaf scale. *Agric. For. Meteorol.* 149, 96–105. https://doi.org/10.1016/j.agrformet.2008.07.007

Verrelst, J., Rivera, J.P., van der Tol, C., Magnani, F., Mohammed, G., Moreno, J., 2015. Global sensitivity analysis of the SCOPE model: What drives simulated canopy-leaving sun- induced fluorescence? *Remote Sens. Environ.*, 166, 8–21. https://doi.org/10.1016/j.rse.2015.06.002

Walker, A.P., Beckerman, A.P., Gu, L., Kattge, J., Cernusak, L.A., Domingues, T.F., Scales, J.C., Wohlfahrt, G., Wullschleger, S.D., Woodward, F.I., 2014. The relationship of leaf photosynthetic traits - Vcmax and Jmax - to leaf nitrogen, leaf phosphorus, and specific leaf area: A meta-analysis and modeling study. *Ecol. Evol.,* 4, 3218–3235. https://doi.org/10.1002/ece3.1173